Energy-band dispersion in oriented thin films of pentatriacontan-18-one by angle-resolved photoemission with synchrotron radiation

Nobuo Ueno
Department of Image Science and Technology, Faculty of Engineering, Chiba University, Chiba 260, Japan

Kazuhiko Seki
Department of Materials Science, Faculty of Science, Hiroshima University, Hiroshima 730, Japan

Naoki Sato
Department of Chemistry, College of Arts and Sciences, The University of Tokyo, Meguro, Tokyo 153, Japan

Hitoshi Fujimoto
Institute for Molecular Science, Myodaiji, Okazaki 444, Japan

Tadao Kuramochi
Analysis Center, Chiba University, Chiba 260, Japan

Kazuyuki Sugita
Department of Image Science and Technology, Faculty of Engineering, Chiba University, Chiba 260, Japan

Hiroo Inokuchi
Institute for Molecular Science, Myodaiji, Okazaki 444, Japan
(Received 17 August 1989)

Angle-resolved photoemission spectra were measured using synchrotron radiation for thin films of the pentatriacontan-18-one molecule [$CH_3(CH_2)_{16}CO(CH_2)_{16}CH_3$] with their long axes perpendicular to the substrate surface. At the preparation of the film, careful studies were made on the molecular decomposition due to vacuum evaporation and on molecular orientation in the evaporated thin films by mass spectroscopy, x-ray diffraction, and angle-resolved photoemission. Valence-band dispersion was observed along the long molecular axis. The results demonstrate that the chemical disorder of the C=O group in the CH_2 chain does not affect the band structure so much, and the molecule shows valence-band dispersion similar to the dispersion in an ideal polyethylene chain. Further, we observed a band which was not observed in previous work. It determines the top of the valence band at the Γ point. Comparison with theoretical results indicates that it corresponds to a band of B_1 (B_{2g} at Γ point) symmetry which consists of only C $2p$ atomic orbitals directed along the carbon chain.

I. INTRODUCTION

Angle-resolved ultraviolet photoemission spectroscopy (ARUPS) is a unique method in probing the energy-band dispersion relation $E=E(k)$ of valence bands for a crystal in wide energy range. Such energy-band dispersions are now determined for many metals and semiconductors by this technique using their single crystals.[1-3]

For organic solids, the intermolecular energy-band dispersion due to weak van der Waals interaction is at most 0.1 eV.[4] This is much smaller than the intramolecular dispersion resulting from strong chemical bonds within a molecule formed with regularly repeating units. Thus we have a chance of observing one-dimensional energy-band dispersion in long-chain molecules.

Among a variety of organic solids consisting of long-chain molecules, the electronic structure of polyethylene has been extensively studied, since (i) it is one of the prototype polymers and also the most typical quasi-one-dimensional compound, and (ii) the elucidation of its electronic structure is the basis for understanding not only its electronic and optical properties but also those of many derivative polymers (e.g., vinyl polymers) and molecules with alkyl chain. Various conventional band-structure spectroscopies have been applied to polyethylene and related compounds in order to examine the one-dimensional energy band, but they gave mainly the information on the electronic density of states, and the comparison with their theoretically calculated density of states could not give the direct evidence of the existence of the one-dimensional energy band.[5-10]

On the other hand, there are some experimental difficulties in the determination of the energy-band dispersion in organic molecular solids by ARUPS. Such

measurements require uniaxially oriented samples, and the use of crystals is hindred by (i) severe charging for compounds of poor conductivity, and (ii) difficulties in preparing large crystals for conductive compounds. Therefore, much effort has been made on the use of oriented thin films of long-chain molecules for such an investigation.[11–15]

Recently, Seki *et al.* and Ueno *et al.* have reported the direct observation of an energy-band dispersion in long-alkyl-chain molecules by ARUPS using thin films of hexatriacontane [$CH_3(CH_2)_{34}CH_3$] (Refs. 12 and 13) and Langmuir-Blodgett (LB) films of cadmium arachidate [$\{CH_3(CH_2)_{18}COO^-\}_2Cd^{2+}$].[13,14] For both films, the molecules are oriented with their long axes perpendicular to the substrate surface. In these works, the main purpose was detecting the one-dimensional energy band along the individual CH_2 chains. Although these experiments could not cover the whole Brillouin zone due to the limitation of available photon energies ($\lesssim 54$ eV), the evidence of the quasi-one-dimensional energy-band dispersion was observed for the first time. The dispersion over the whole Brillouin zone was observed more recently for $CH_3(CH_2)_{34}CH_3$ by Fujimoto *et al.* using photon energies up to 75 eV.[15] However, at the top portion of the valence bands, which is important in discussing the electronic properties, these works could not detect the highly dispersive B_1 band (B_{2g} symmetry at the Γ point) predicted by theoretical band calculation.

Another important subject for understanding this class of compounds is the determination of the minimum number of successive CH_2 units required for the appearance of the energy band characterized by a dispersion relation,[16,17] including the investigation of the effects of the chain ends or the chemical disorder in a chain on the band formation within the molecules. We expect that this kind of information would also help the understanding of the electronic structure and properties of systems with finite units, e.g., fine particles, clusters, and ultrathin films of molecules.

In the present work, we have investigated these two points, i.e., (i) more extensive study of the topmost valence band, and (ii) a study of the effect of a chemical disorder on the valence-band structure of CH_2 chain by the ARUPS study of pentatriacontan-18-one, $CH_3(CH_2)_{16}CO(CH_2)_{16}CH_3$. It contains the chemical disorder by a C=O group at the center of the chain, and has only 16 successive CH_2 units which are shorter than the previously studied molecules.[12–15] Further, we used photon energies up to 120 eV for finding the missing topmost band.

In the following we describe (i) the preparation of oriented thin film of pentatriacontan-18-one by vacuum evaporation with a careful examination of stability of the molecules at vacuum evaporation and the molecular orientation in the evaporated thin films, and (ii) the results of ARUPS measurements with synchrotron radiation for the well-characterized films. The results demonstrate that the quasi-one-dimensional energy bands similar to those in an ideal polyethylene chain [$(CH_2)_\infty$] can be observed even for pentatriacontan-18-one molecule, and the top of the valence bands is actually located at the Γ point by a highly dispersive band as predicted by theoretical calculations.

II. EXPERIMENTAL

A. Measurements

The ARUPS measurements were carried out at the beam line 8B2 of the UVSOR storage ring at Institute for Molecular Science. The synchrotron radiation from the storage ring, operated at a ring current of < 100 mA, was monochromatized by a plane-grating monochromator.[18] The photon energies up to 120 eV were used.

The photoelectron spectrometer consists of a sample preparation chamber, a measurement chamber, and a sample transfer system. Energy analysis of photoelectrons was performed with a hemispherical analyzer of 25-mm mean radius, which can be rotated around vertical and horizontal axes.[19] The photoelectron spectra were recorded under the total resolution of about 0.2–1 eV, depending on the photon energy $h\nu$ and the potential setting of the analyzer. The spectra measured at low and high resolution were very similar due to the broadness of spectral features.

When the sample was irradiated by intense synchrotron radiation, the spectrum changed rapidly due to the radiation damage. In order to minimize the damage, the incident light intensity was reduced by introducing a nickel mesh of 50% nominal transmission between the monochromator and the measurement chamber when the storage-ring current was greater than 50 mA. A typical count rate was about 500 cps at $h\nu = 100$ eV under a total resolution of about 1 eV for the most intense band. Scanning a spectrum of about 25-eV width required several hours around this photon energy. Even under such low photon flux, the spectrum changed after repeated measurements. Therefore we changed sampling position of the specimen after every two or three spectra. By such careful measurements, we could obtain the spectra amenable for the subsequent analysis.

The experimental parameters for the ARUPS measurements are depicted in Fig. 1. As in the case of previous

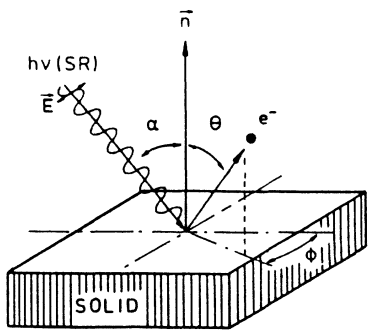

FIG. 1. Parameters of angle-resolved UPS measurements. α, incidence angle of synchrotron radiation (SR); θ, polar emission angle of photoelectrons; and ϕ, azimuthal emission angle of photoelectrons. The electric vector of the synchrotron radiation is on the plane of $\phi = 0$ and perpendicular to the surface. In the present experiment, ϕ was fixed at 0.

studies,[12,13,15] uniaxially oriented samples required for the determination of energy-band dispersion by ARUPS were obtained by vacuum evaporation. In these films, the molecules are oriented with their long axes perpendicular to the substrate surface, and the energy-band dispersion was determined by studying the $h\nu$ dependence of the photoelectron spectra for electrons emitted normal to the surface ($\theta=0°$). The details of the sample preparation and characterization are described below.

B. Preparation and characterization of oriented thin films

The sample of pentatriacontan-18-one was commercially obtained from Tokyo Kasei Kogyo Co. Ltd., and was purified by two reprecipitations with toluene and methanol. Before *in situ* preparation of evaporated thin films for the ARUPS measurements, we studied the condition of the evaporation for the perpendicular orientation of the molecules without decomposition.

In Fig. 2, we show typical mass spectra of vaporized pentatriacontan-18-one at different heating temperatures using a mass spectrometer (Hitachi M-60). The spectra were obtained as a function of time after introducing the sample crystal in a quartz evaporation cell into the heating furnance kept at 150 °C. The temperature of the crystal increased with time and reached 150 °C after about 5 min. The evaporated molecules were ionized by 70-eV electron bombardment and the temperature of the ionization chamber was also maintained at 150 °C. The observed mass spectra include the contribution from the products of decomposition caused by the electron ionization. It is clearly seen, however, that the mass peaks of decomposed species relative to the undecomposed parent ions ($M/z=506$) become stronger at high temperature. Further, the decomposition of the molecule occurs mainly by a bond scission at one side of the C=O group: $CH_3(CH_2)_{16}CO(CH_2)_{16}CH_3 \rightarrow CH_3(CH_2)_{n<16}+(CH_2)_{16-n}+CO(CH_2)_{16}CH_3$ ($M/z=267$). Using these results, we plotted the intensity ratio of mass peaks between the parent ions and selected fragment ions, i.e., [I(43,57,71)/I(506,507)] and [I(267)/I(506,507)], where $I(x,y,z)$ indicates the sum of the intensity of mass peaks for $M/z=x$, $M/z=y$, and $M/z=z$. That is, I(506,507) is the intensity of the undecomposed ions, and the others are the integrated intensity of selected fragment ions. The results are also shown in Fig. 2(b). It indicates an increased decomposition at high temperature besides the decomposition by electron impact. The increase of I(43,57,71)/I(506,506) at small scan number (e.g., scan number 15, time 1.1 min) is due to organic contaminants released from the evaporation cell which vaporize at low temperature. From these experiments, we can conclude that the molecules are not so stable against the vacuum evaporation at high temperature and the evaporation at low temperature is necessary for preparing thin films with little decomposition.

Figure 3 displays the x-ray diffraction pattern of a film of pentatriacontan-18-one evaporated onto a copper substrate at room temperature with a deposition rate of 4 Å/min using the evaporation cell reported elsewhere.[20] The film thickness was 900 Å. The distance between the substrate and the evaporation cell was about 10 cm. In the figure, we also show the x-ray diffraction pattern of melt-grown polycrystal (nonvertical orientation) and vertically oriented polycrystal obtained by rubbing small crystals over an adhesive substrate. The sharp (00l) diffractions are clearly observed for the evaporated film prepared with the above-described evaporation conditions. Thus the vertically oriented films could be obtained by the vacuum evaporation with little molecular decomposition.

The ARUPS measurements require oriented thin films of thickness less than 100 Å in order to avoid the charg-

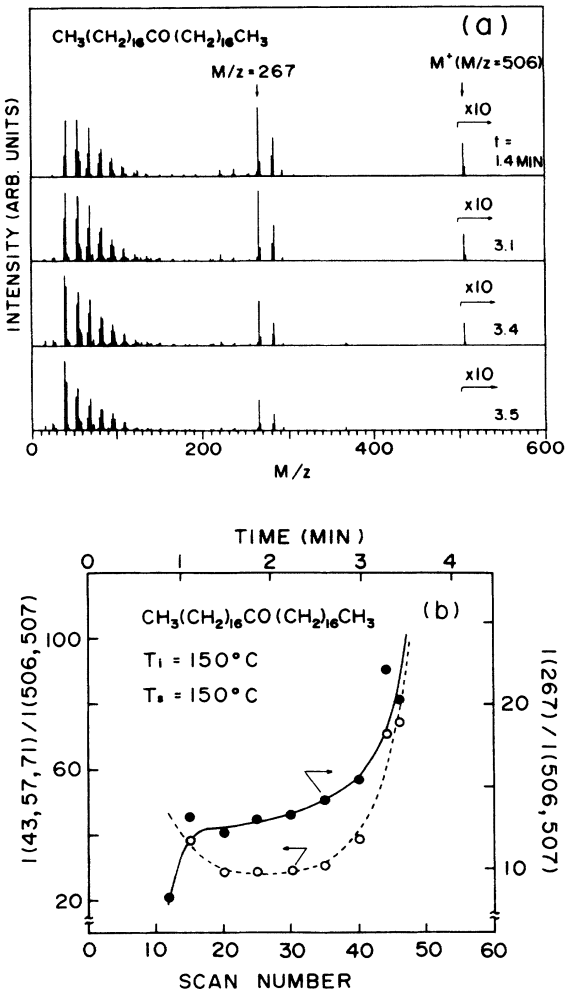

FIG. 2. Examples of mass spectra of pentatriacontan-18-one during vacuum evaporation at (a) different evaporation temperature and (b) the dependence of molecular decomposition on the evaporation temperature. In (a), t indicates the time from the beginning of the mass measurements, and the intensity is 10 times enlarged above $M/z=500$. The sample temperature increases with t (see text). Molecular weight of pentatriacontan-18-one is 506. The fragment of $M/z=267$ corresponds to $CO(CH_2)_{16}CH_3^+$. For (b), the abscissa (scan number, time) corresponds to the temperature of the sample, and the ordinate shows the intensity ratio between the fragment and the parent ions. The temperature at 3.5 min (scan number 45) was estimated to be 140 °C. The melting point of the crystal is 86–87 °C.

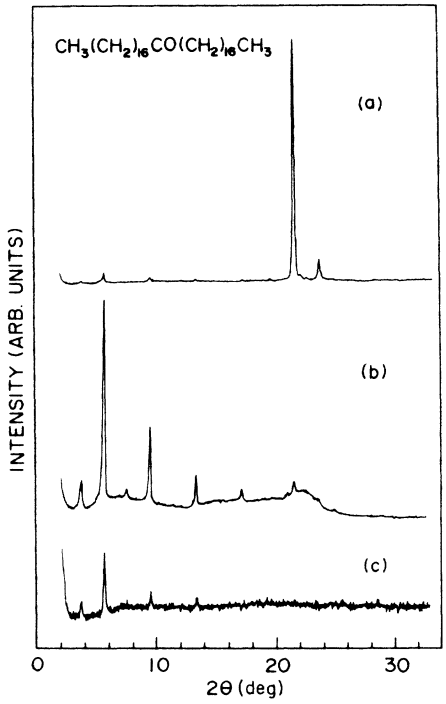

FIG. 3. X-ray diffraction patterns of pentatriacontan-18-one prepared in different ways. (a) Melt-grown polycrystals (without vertical orientation). (b) Oriented polycrystals prepared by rubbing the crystals over an adhesive substrate, showing vertical orientation of the molecules to the substrate surface. (c) Evaporated thin film (thickness of 900 Å, deposition rate of 4 Å/min). Cu Kα x ray was used.

ing of the film during the measurements. We prepared 86–98-Å-thick films (~2 layers) on a molybdenum substrate at room temperature with the same evaporation cell and deposition rate as described above in the preparation chamber of a pressure below 5×10^{-8} Torr. After the film deposition, the specimen was immediately transferred to the measurement chamber of a pressure of $\sim10^{-10}$ Torr. All measurements were perfomed at room tempeature.

The orientation of the molecules in the ultrathin film was confirmed by measuring the dependence of the ARUPS spectra on the emission angle θ (see Fig. 1). As an example, the θ dependence of the spectra at $h\nu=35$ eV is shown in Fig. 4 for $\theta=0°$ and 60° at the incidence angle of the photons $\alpha=70°$. In the figure, the θ dependence of the spectra for oriented and unoriented LB films of cadmium arachidate[13] are also shown for comparison. The large θ dependence of the spectra for the present specimen, which is similar to the θ dependence for the oriented LB films, indicates that the vertical orientation of the molecules could be realized in the ultrathin film (~90 Å) as well as in the thicker films (900 Å). We note in passing that the absence of serious broadening of the ARUPS features for increasing θ indicates a small intermolecular energy-band dispersion in these films.

In summarizing the above, we prepared vertically oriented films of pentatriacontan-18-one with a careful study of the evaporation condition and the molecular orientation, and they were used for the determination of the energy-band dispersion from the $h\nu$ dependence of the normal emission spectra.

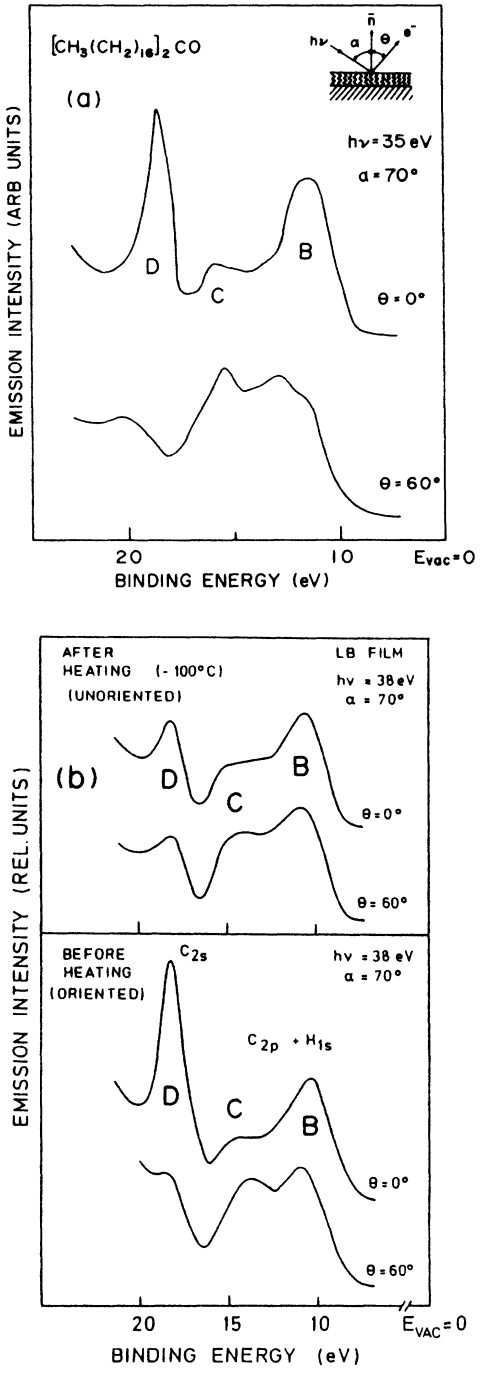

FIG. 4. (a) Dependence of the photoelectron spectra of pentatriacontan-18-one for $h\nu=35$ eV on the emission angle θ. (b) For comparison, θ dependence of the photoelectron spectra of oriented and unoriented Langmuir-Blodgett films of cadmium arachidate (Ref. 13) are also shown.

III. RESULTS AND DISCUSSION

A. Photon energy dependence of normal emission spectra

In Fig. 5, we display the $h\nu$ dependence of the spectra for photoelectrons emitted normal ($\theta=0°$) to the surface at $\alpha=70°$ in the $h\nu$ range of $40 \lesssim h\nu \lesssim 120$ eV. The spectra are dominated by the contribution from the alkyl chain and not affected appreciably by the chemical "impurity" C=O group in the chain. Similar results were obtained in our previous studies where the spectra of LB films of cadmium arachidate[13,14] gave very similar spectra with those of hexatriacontane.[12,13] This is ascribed to (i) a small effect of the C=O group on the band structure of the CH_2 chain, (ii) the short electron mean free path (<20 Å) in the present kinetic-energy range of photoelectrons[21–23] compared to the length of alkyl part near the surface (~ 20 Å) of the oriented film, and (iii) the small ratio of valence electrons involved in the C=O parts (10 electrons) to those in the alkyl parts $(CH_2)_{16}$ (96 electrons). Further, we could not observe clear evidence of the nondispersive photoelectron features from the CH_3 end group covering the surface. At $h\nu > 108$ eV, we observed a shoulder *F*. At present, however, it is uncertain whether this shoulder can be ascribed to the end CH_3 group.

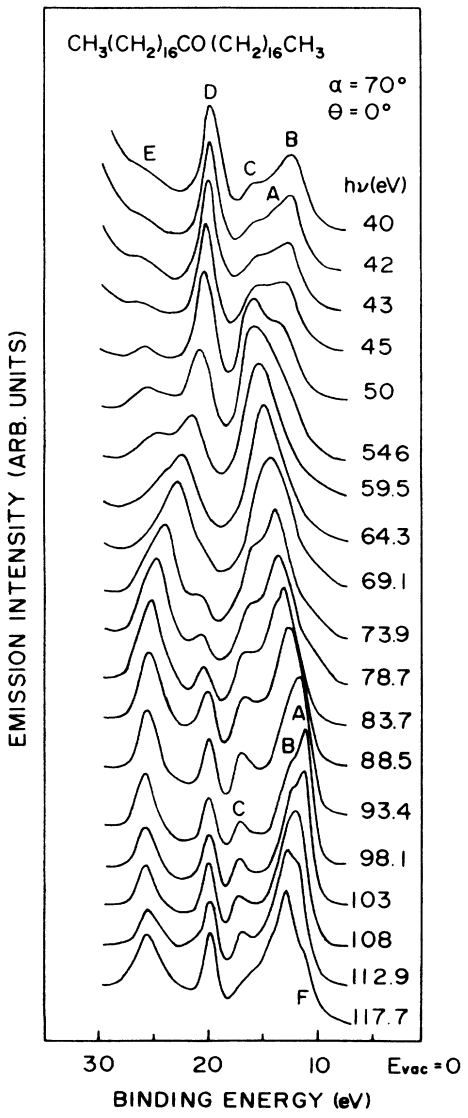

FIG. 5. Photon-energy dependence of the normal-emission photoelectron spectra of vertically oriented thin films of pentatriacontan-18-one for $\alpha=70°$.

The main spectral features show continuous but drastic changes both in peak positions and peak intensities. The deep-lying features *D* and *E*, which correspond to the bands derived from C 2*s* and H 1*s* atomic orbitals (see next section), become closer with increasing $h\nu$, merge into a single peak around $h\nu=65$ eV, and again split into two peaks above $h\nu=65$ eV. As discussed later, this is the result of the crossing of the two bands at the boundary of the Brillouin zone (*X* point).

On the other hand, the features *A*, *B*, and *C*, which originate in the bands derived C $2p$+H 1*s* orbitals (see next section), also show remarkable change in their energy positions at high photon energies. The large $h\nu$ dependence of the low-lying valence band above 70 eV was not observed in the previous work using lower photon energies.[12–15] For example, these bands give only two main features *B* and *C* at $h\nu=40$ eV. At $h\nu \simeq 42$ eV a new peak *A* appears and at $h\nu \simeq 64$ eV these features *A*, *B*, and *C* form a skewed single peak. This skewed feature suggests the bands giving features *A* and *C* join at a value of the momentum k and the band for feature *B* locates at a little lower binding-energy position at this k value. For $h\nu > 64$ eV, this skewed peak starts to split into three peaks again with an increase in $h\nu$. The feature *A* becomes sharper and gives the lowest binding energy in all the spectra at $h\nu=98$–103 eV. The drastic change in intensity can be ascribed to the increase of the optical transition probability at higher $h\nu$ region. It is noticeable that the highly dispersive feature *A* was observed and it determines the top of the valence bands rather than the feature *B* which is at the top for lower $h\nu$. As is shown in the next section, these changes can be seen more clearly by plotting the energy-band dispersion relation. The results indicate that for long alkyl compounds the use of high photon energies is very effective in probing the valence-band dispersion.

B. Intramolecular energy-band mapping

For the determination of the energy-band dispersion $E=E(k)$ along the long molecular axis from the normal-emission spectra in Fig. 5, we follow the procedure described in more detail in the previous paper.[13] We assume that (i) the photoemission process is expressed by the three-step model,[24] (ii) both the energy and the momentum are conserved for the optical transitions of electrons, and (iii) the final state is expressed by a free-electron-like parabola ($m^*/m_0=1$), where m^* and m_0 are the effective mass of the electron and the free-electron mass, respectively. Briefly, we use the following relations:

$$E_i = E_k - h\nu \tag{1}$$

$$k_i^{\perp} = k_f^{\perp} = [2m_0(E_f - V_0)]^{1/2}/\hbar\,, \tag{2}$$

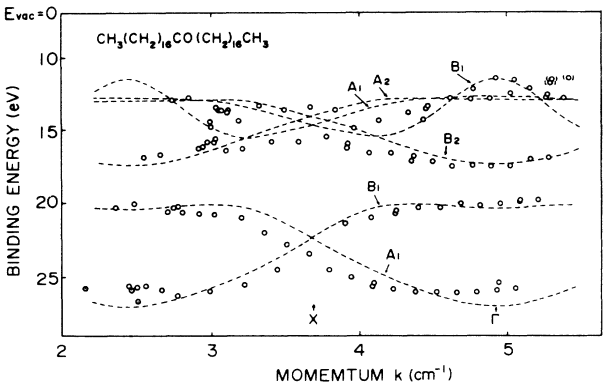

FIG. 6. Energy-band dispersion along the long molecular axis of $CH_3(CH_2)_{16}CO(CH_2)_{16}CH_3$ in the extended zone scheme. The experimental results are indicated by the open circles. The theoretical band structure for infinite length of CH_2 chain calculated by Karpfen (Ref. 28) with some modification (see text) is also shown by dashed lines. Points in parentheses correspond to the features F in Fig. 5 (see text).

where k_i, k_f, E_i, and E_f are the wave vectors and the energies of the electron before and after photoexcitation in the solid, E_k is the kinetic energy of the emitted free electron, and the energies are referred to the vacuum level. The component normal to the surface is denoted by $\perp$. V_0 is the constant inner potential in the solid for the final free-electron-like parabola. In the present study, we used $V_0 = -5.5$ eV, which was determined for LB films of cadmium arachidate,[14] since the low-energy electron transmission experiments on pentatriacontan-18-one gave similar conduction-band features[25] with those of hexatriacontane[26] and the LB films[27] at high-energy region.

Using normal emission spectra and Eqs. (1) and (2), we can calculate the binding energy of the valence band E_B $(= -E_i)$ and momentum k_i, and the results are shown in Fig. 6 using extended zone scheme, where the points of larger k were obtained using the spectra measured with higher $h\nu$. They include many other data not shown in Fig. 5. In the figure, the result of theoretical band calculation for an ideal infinite CH_2 chain by Karpfen[28] is also shown for comparison. The energy scale of the theoretical result is contracted by 0.8 times as in the previous work[12-15] and shifted for the best fit with the experimental results. The symmetry of the energy bands for the ideal chain is also shown after McCubbin[29] and Falk and Fleming.[30]

In the plot of experimental data, we note at first that the binding-energy position shifts continuously with increasing momentum k. Further, the band crossing at the boundary of the Brillouin zone (X point) is seen. Judging from the good agreement between the ARUPS and the theoretical results, we conclude that the energy bands characterized by the momentum k exist along the long axis of pentatriacontan-18-one.

C. Bands derived from carbon 2s and hydrogen 1s orbitals

The deep-lying two bands of A_1 and B_1 symmetry primarily consist of C $2s$ orbitals with some mixture of H $1s$ orbitals.[29,30] These two bands give the features D and E in the photoelectron spectra. The simple nature of these bands is useful in discussing the effect of the chemical "impurity" on the band structure as well as the chain-length dependence of the band. As seen from Fig. 6, the experimentally obtained energy-band dispersion agrees very well with the theoretical one for an ideal infinite chain. The agreement indicates that the energy-band dispersion is dominated by a short-range interaction along the chain. This idea is supported by a fact that the theoretical band dispersion also showed close agreement with the dispersion estimated by plotting the observed binding energies of n alkane oligomers with the momentum k for each level calculated by a simple tight-binding model with nearest-neighbor interaction.[13] This in turn suggests that O $2s$ atomic orbital is localized at the chemical disorder. The localization of O $2s$ atomic orbital in pentatriacontan-18-one is also expected from the molecular orbital (MO) calculations[31] for acetone (CH_3COCH_3), where O $2s$ atomic orbital is mainly localized at C=O bond. Further, C $2s$-derived molecular orbitals in acetone show close resemblance to those in propane ($CH_3CH_2CH_3$).[31] It is considered that the C $2s$ orbital of the chemical disorder, C=O, in pentatriacontan-18-one behaves as that of the CH_2 part. The C=O groups in different molecules do not interact strongly, and we can regard them as isolated "impurities." We can thus expect that the C=O part will not affect the band structure of the CH_2 chain, but form localized "impurity" levels which could not be observed in the present experiment by the reason described previously.

Another important point in comparing the band structures of infinite and finite chains is the breakdown of the translational symmetry in the finite chain. For example, the degeneracy at the X point for an ideal infinite chain is lifted by introducing chemical disorder and/or chain ends due to the elimination of the glide symmetry.[29] Since our experiments do not indicate such a separation, the splitting is probably small.

D. Bands derived from carbon 2p and hydrogen 1s orbitals

The upper A_1 and B_1 bands and A_2 and B_2 bands consist of C $2p$ and H $1s$ orbitals. These bands give the features A, B, and C in the photoelectron spectra. Again the experimental and theoretical results agree fairly well. In particular, the highly dispersive upper B_1 band near the Γ point is clearly observed. This band was not observed in the previous work[12-15] where lower $h\nu$ was used. This agreement indicates the correctness of theoretical calculations, which claims that (i) the top of the valence bands is located at the Γ point, (ii) it is determined by this B_1 band, and (iii) at the Γ point this band has B_{2g} symmetry and consists only of C $2p_x$ orbitals.[29,30] The results correspond well to those of ESR and intermediate-neglect-of-differential-overlap–molecular-orbital (INDO/MO) studies of the ground state of shorter n-alkane cations by Toriyama *et al.*[32]

Although it is difficult to discuss the effects of the chemical disorder, C=O, on these bands, the good agreement between the experimental result and the

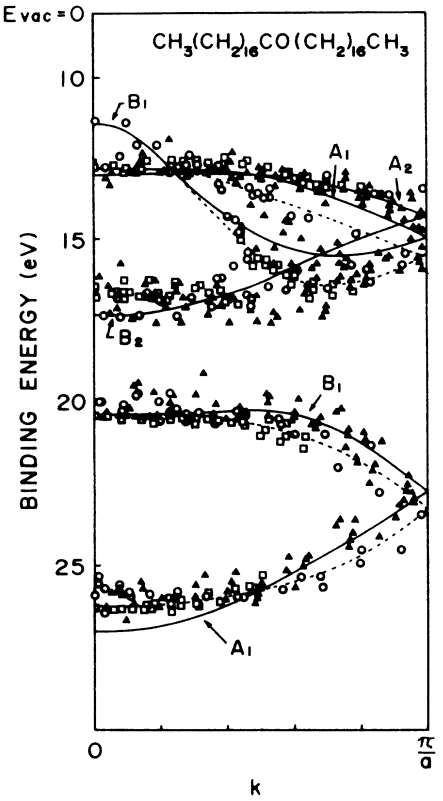

FIG. 7. Comparison of experimental energy-band dispersions for pentatriacontan-18-one, hexatriacontane, and Langmuir-Blodgett films of cadmium arachidate in reduced zone scheme. ○, pentatriacontan-18-one, $CH_3(CH_2)_{16}CO(CH_2)_{16}CH_3$ (present results); △, hexatriacontane (Refs. 12 and 13) $CH_3(CH_2)_{34}CH_3$; ▲, hexatriacontane (Ref. 15); □, Langmuir-Blodgett films of cadmium arachidate (Refs. 13 and 14), $[CH_3(CH_2)_{18}COO^-]_2Cd^{2+}$. The theoretical result by Karpfen (Ref. 28) is shown by a solid curve with some modification (see text). The dotted curves indicate the experimentally deduced dispersion curves for the A_1 and B_1 bands.

theoretical one for the infinite CH_2 chain leads to a conclusion that (i) the C=O parts can be considered to be "impurities" as in the case of C $2s$+H $1s$ derived bands, or (ii) 16 successive CH_2 units can give an energy-band dispersion similar to that in the infinite CH_2 chain.

On the other hand, as in the case of (C $2s$+H $1s$)-derived bands the expected splitting at the X point could not be observed, probably for a similar reason to the C $2s$+H $1s$ bands.

E. Comparison with other experimental results

The comparison between the present results and those for hexatriacontane[12,13,15] and LB films of Cd arachidate[13,14] is shown in Fig. 7, in the reduced zone scheme. The energy axes of the previous results are slightly shifted to fit the upper C $2s$+H $1s$ band at the Γ point with the present result. The four independent experimental results for different molecules of various CH_2 chain length agree reasonably well.

From the comparison between the experimental and theoretical results, it seems that the A_1 and B_1 bands should be at larger binding-energy positions than the theoretical result as shown by the dotted curves.

Recently, Springborg and Lev[33] calculated the valence-band dispersion of polyethylene with a first-principles, density-functional method. The present result also showed good agreement with their dispersion relation.

IV. SUMMARY

We have measured the energy-band dispersion relation along the long molecular axes of pentatriacontan-18-one, $CH_3(CH_2)_{16}CO(CH_2)_{16}CH_3$, using well-characterized evaporated thin films with vertical orientation of the molecules. Further, on the way of sample preparation, the molecular decomposition during vacuum evaporation and the molecular orientation of the evaporated thin films were studied by mass spectroscopy, x-ray diffraction, and angle-resolved photoemission.

At low evaporation temperature pentatriacontan-18-one can be evaporated with little molecular decomposition to form ultrathin film on a metal substrate with their long axes perpendicular to the substrate surface.

The results clearly demonstrate that (i) the quasi-one-dimensional energy-band dispersion similar to the dispersion in polyethylene chain exists even in the molecule which has only 16 successive CH_2 units due to the existence of the chemical "impurity," C=O, at the center of the molecule. They confirm the theoretical calculation predicting that the top of the valence bands in the CH_2 chain is determined by the highly dispersive upper B_1 band at the Γ point.

ACKNOWLEDGMENTS

The authors are very grateful to the staff of UVSOR at Institute for Molecular Science for their support. N.U. and K.S. deeply thank the late Professor E. E. Koch of Berliner Elektronenspeicherring-Gesellschaft für Synchrotronstrahlung m.b.H. (BESSY) for his constant interest and encouragement. H.F. is grateful to the Japan Society for the Promotion of Science and the Toyoda Physical and Chemical Research Institute for partial financial support. One of us (N.U.) acknowledges the support from a Grant-in-Aid for Scientific Research (No. 63550005) from the Ministry of Education, Science and Culture of Japan. This work was performed as a part of Joint Studies Program (1987–1990) of IMS-UVSOR Facility.

[1]F. J. Himpsel and N. V. Smith, in *Handbook of Synchrotron Radiation,* edited by E. E. Koch (North-Holland, Amsterdam, 1983), Vol. 1b, p. 905.

[2]F. J. Himpsel, Adv. Phys. **32**, 1 (1983).

[3]F. J. Himpsel, Appl. Opt. **19**, 3964 (1980).

[4]See, for example, M. Pope and C. E. Swenberg, *Electronic Process in Organic Crystals* (Clarendon, Oxford, 1982).

[5]M. H. Wood, M. Barber, I. H. Hiller, and J. M. Thomas, J.

Chem. Phys. **56**, 1788 (1972).
[6]J. Delhalle, J.-M. Andre, S. Delhalle, J. J. Pireaux, R. Caudano, and J. J. Verbist, J. Chem. Phys. **60**, 595 (1974).
[7]K. Seki, S. Hashimoto, N. Sato, Y. Harada, K. Ishii, H. Inokuchi, and J. Kanbe, J. Chem. Phys. **66**, 3644 (1977).
[8]N. Ueno, T. Fukushima, K. Sugita, S. Kiyono, K. Seki, and H. Inokuchi, J. Phys. Soc. Jpn. **48**, 1254 (1980).
[9]N. Ueno and K. Sugita, Solid State Commun. **34**, 355 (1980).
[10]N. Ueno, K. Sugita, and S. Kiyono, Chem. Phys. Lett. **82**, 296 (1981).
[11]K. Seki and H. Inokuchi, Chem. Phys. Lett. **89**, 268 (1982).
[12]K. Seki, U. Karlsson, R. Engelhardt, and E. E. Koch, Chem. Phys. Lett. **103**, 343 (1984).
[13]K. Seki, N. Ueno, U. O. Karlsson, R. Engelhardt, and E. E. Koch, Chem. Phys. **105**, 247 (1986).
[14]N. Ueno, W. Gaedeke, E. E. Koch, R. Engelhardt, R. Dudde, L. Laxhuber, and H. Moehwald, J. Mol. Electron. **1**, 19 (1985).
[15]H. Fujimoti, T. Mori, H. Inokuchi, N. Ueno, K. Sugita, and K. Seki, Chem. Phys. Lett. **141**, 485 (1987).
[16]J. J. Pireaux, S. Svensson, E. Basilier, P.-A. Malmqvist, U. Gelius, R. Caudano, and K. Siegbahn, Phys. Rev. A **14**, 2133 (1976).
[17]J. J. Pireaux and R. Caudano, Phys. Rev. B **15**, 2242 (1977).
[18]K. Seki, H. Nakagawa, K. Fukui, E. Ishiguro, R. Kato, T. Mori, K. Sakai, and M. Watanabe, Nucl. Instrum. Methods A **246**, 264 (1986).
[19]K. Seki, H. Fujimoto, T. Mori, and H. Inokuchi, UVSOR Activity Reports, 1986, p. 11 (unpublished).
[20]N. Sato, K. Seki, and H. Inokuchi, Rev. Sci. Instrum. **58**, 1112 (1987).
[21]See, for example, M. P. Seah and W. A. Donch, Surf. Interface Anal. **1**, 2 (1979).
[22]E. Cartier and P. Pfluger, Phys. Rev. B **34**, 8822 (1986).
[23]E. Cartier, P. Pfluger, J.-J. Pireaux, and M. Rei Vilar, Appl. Phys. A **44**, 43 (1987).
[24]C. N. Burglund and W. E. Spicer, Phys. Rev. A **136**, 1030 (1964).
[25]N. Ueno *et al.*, unpublished.
[26]N. Ueno, K. Sugita, K. Seki, and H. Inokuchi, Phys. Rev. B **34**, 6386 (1986).
[27]N. Ueno, H. Nakahara, K. Sugita, and K. Fukuda, Thin Solid Films (to be published).
[28]A. Karpfen, J. Chem. Phys. **75**, 238 (1981).
[29]W. L. McCubbin, in *Electronic Structure of Polymers and Molecular Crystals,* edited by J-M. Andre and J. Ladik (Plenum, New York, 1974), p. 171, and references therein.
[30]J. E. Falk and R. J. Fleming, J. Phys. C **6**, 2954 (1973).
[31]See, for example, W. L. Jorgensen and L. Salem, *The Organic Chemist's Book of Orbitals* (Academic, New York, 1973).
[32]K. Toriyama, K. Nunome, and M. Iwasaki, J. Chem. Phys. **77**, 5891 (1982).
[33]M. Springborg and M. Lev, private communication.